Structure and gas permeability of siloxane–imide block copolymer membranes: 1. Effect of siloxane content

Y. Tsujita*, K. Yoshimura, H. Yoshimizu, A. Takizawa and T. Kinoshita
Department of Materials Science and Engineering, Nagoya Institute of Technology, Gokiso-cho, Showa-ku, Nagoya 466, Japan

and M. Furukawa, Y. Yamada and K. Wada
Nippon Steel Chemical Co. Ltd, Nakabara, Tobata-ku, Kita-kyushu 804, Japan
(Received 20 May 1992; revised 9 September 1992)

Siloxane–imide block copolymer membranes with various siloxane contents were prepared and their dynamic viscoelasticity, sorption of carbon dioxide, and permeability of carbon dioxide, oxygen and nitrogen were studied. The siloxane–imide block copolymer consists of a microphase separated structure of imide-rich and siloxane phases, and the mechanical properties of the siloxane–imide block copolymer are well retained up to a siloxane content of about 20 wt%. The amount of carbon dioxide sorbed into the siloxane–imide block copolymer decreases with the introduction of siloxane, reflecting the less-sorptive capability of the siloxane group. The sorption behaviour of the block copolymers is interpreted in terms of a dual-mode sorption theory, which is applied to glassy imide-rich phases. On the other hand, the permeability coefficients of carbon dioxide, oxygen and nitrogen are remarkably increased with siloxane content when the latter is more than 10 wt%, and the permselectivity of oxygen to nitrogen is decreased with siloxane content. These behaviours are interpreted by considering the arrangement of the two phases in the membrane.

(Keywords: siloxane–imide block copolymer; permeability; sorption; permselectivity; phase separation)

INTRODUCTION

Oxygen and nitrogen separation characteristics of polymer membranes have been studied extensively over the years for applications in medicine and combustion. Poly(dimethyl siloxane) (PDMS)[1,2] and its derivatives[3–6] have been reported to have a high O_2 permeability owing to their high diffusion, but have relatively low permselectivity of O_2 to N_2 and poor thin-film formability. On the contrary, glassy polymers have, in general, a high permselectivity of O_2 to N_2 and are also interesting because of their better thin-film formability and heat stability, even though the magnitude of the permeability coefficient is comparatively low. To obtain a polymer membrane that has the advantages of both PDMS and glassy polymers, a block copolymer has been designed. For example, block copolymer membranes of PDMS and polycarbonate[3] or poly(vinylphenol)[4] have been reported elsewhere to improve the poor thin-film formability of PDMS. In particular, thermally stable polymer membranes are necessary for gas separation systems at high temperature. Since polyimides (PI) have high glass transition temperature (T_g), excellent mechanical and thermal stability, and high permselectivity[7–15], it can be expected that block copolymer membranes of PDMS and PI are more thermally stable and highly gas-permeable membranes.

In this study, siloxane–imide block copolymer membranes with various PDMS contents were prepared and their dynamic viscoelasticity, sorption of CO_2, and permeability of CO_2, O_2 and N_2 were studied in order to reveal the relationship between the PDMS content and their structure and permeability.

EXPERIMENTAL

Materials

Siloxane–amic acid block copolymers (Si*xx*–PAA) with various PDMS contents (*xx* wt%) were prepared from aromatic tetracarboxylic acid dianhydride, aromatic diamine and diamine–PDMS, as shown in *Scheme 1*, as the prepolymer of the siloxane–imide block copolymers (Si*xx*–PI). In the present paper, PDMS with a mean degree of polymerization of 7.6 was used, and the PDMS contents of the copolymers were varied by changing the molar ratio of aromatic tetracarboxylic acid dianhydride and aromatic diamine to diamine–PDMS. Si*xx*–PAA membranes were prepared by casting their *N*-methylpyrrolidone/2-methoxyethyl ether (7/3 v/v) solution on a Teflon plate at room temperature. Si*xx*–PI membranes were obtained from the imidization of Si*xx*–PAA membranes, which was carried out by curing at 240°C for 48 h *in vacuo*. Poly(amic acid) (Si0–PAA) and polyimide (Si0–PI) membranes were similarly polymerized and prepared to obtain reference data.

* To whom correspondence should be addressed

0032-3861/93/122597-05

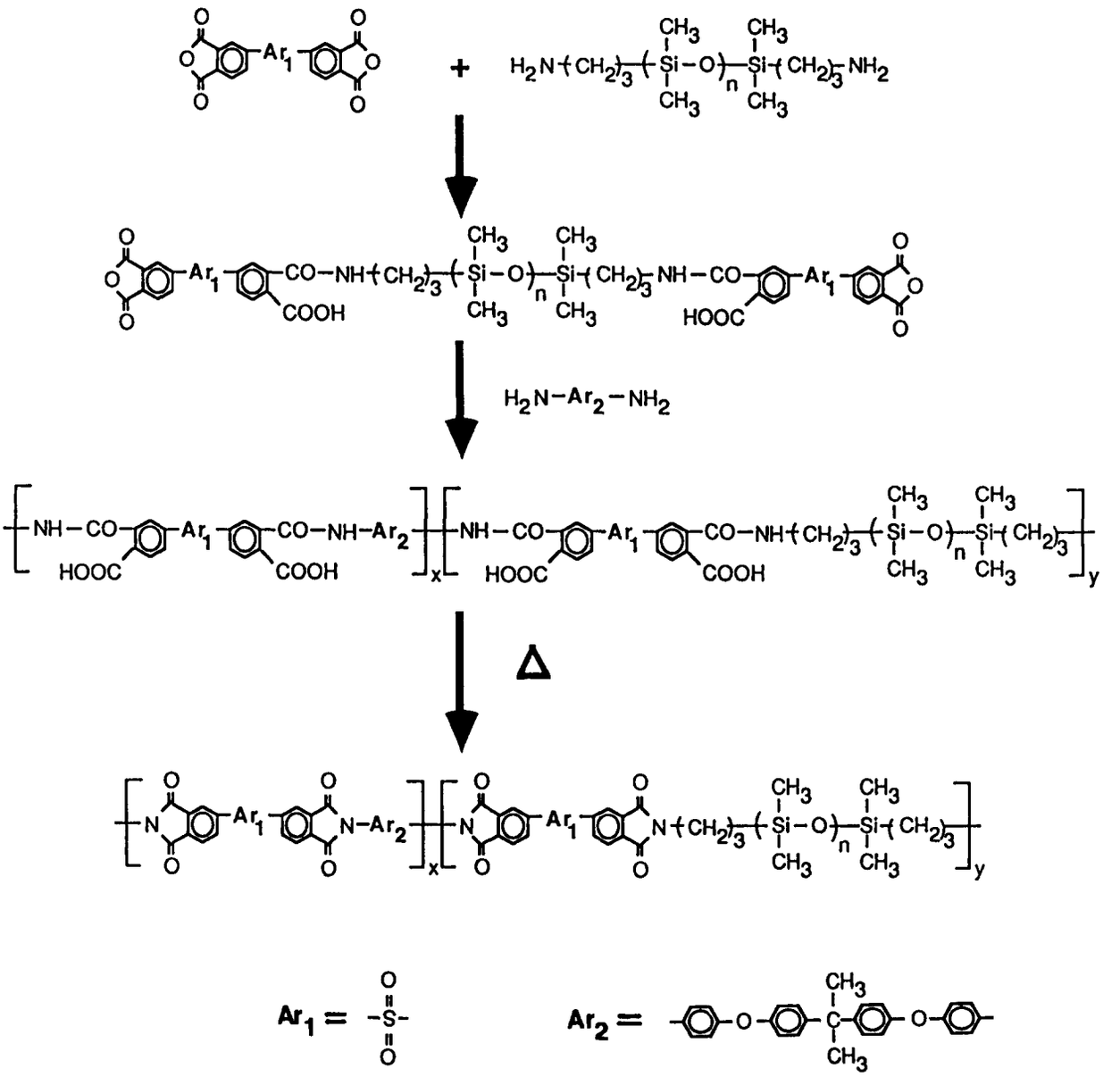

Scheme 1

Thicknesses of all the membranes were in the range of 50 to 100 μm.

CO_2, O_2 and N_2 used in this study are at least 99.9% pure and were used without further purification.

Methods

Dynamic mechanical properties over the temperature range of -150 to 300°C at a heating rate of 2°C min^{-1} were measured using a DMS100 Dynamic Mechanical Spectrometer from Seiko Instruments Inc. Membranes were scanned with an imposed frequency of 10 Hz in the shear mode.

CO_2 sorption measurements were carried out at 25°C by using a gravimetric sorption apparatus with an electromicrobalance (Type-2000, Cahn Instruments Inc.). After sufficient drying of the membranes under about 10^{-4} mmHg, the weight increase due to sorption of gas in the membranes under a fixed pressure was recorded and the net amount sorbed was corrected by subtracting a buoyancy contribution.

The measurements of the permeability coefficients were performed according to the following procedure. The membrane mounted in a permeation cell sealed with a Teflon ring (the permeable area is 1.887 cm^2) was degassed for 24 h at 10^{-4} mmHg in a permeation apparatus. The downstream side of the membrane was evacuated to about 10^{-4} mmHg. Permeant gas was introduced on the upstream side, and the permeant pressure on the downstream side was monitored using an MKS-Baratron pressure transducer (227AA). The permeability coefficient was evaluated from steady-state gas permeation rate.

RESULTS AND DISCUSSION

Dynamic mechanical analysis

Figure 1 shows the temperature dependences of shear modulus (G') and loss tangent ($\tan\delta$) for Si0–PI, Si10–PI, Si20–PI and Si30PI membranes. Two peaks are observed in the tan δ curves for Si*xx*–PI membranes, while only one peak is observed for Si0–PI at about 270°C. The peaks in tan δ observed at 200–270°C, where the values of G' are suddenly decreased in the corresponding G' curves, are assigned to a primary dispersion of the PI-rich phase. In *Figure 1*, the tan δ peak at ca. 130°C, which corresponds to a primary

Table 1 Dual-mode sorption parameters at 25°C and glass transition temperatures of Si0–PAA, Si0–PI, Si20–PAA and Si20–PI membranes

	T_g[a] (°C)	$k_D \times 10^2$[b] (cm^3/cm^3 cmHg)	C'_H[c] (cm^3/cm^3)	$b \times 10^3$[d] ($cmHg^{-1}$)
Si0–PAA	132.5	1.79	9.6	4.03
Si0–PI	268.4	2.29	23.6	7.66
Si20–PAA	−118.0, 133.7	1.84	8.0	3.80
Si20–PI	−106.6, 217.5	2.09	15.3	3.87

[a] T_g = glass transition temperature determined from dynamic mechanical analysis; temperature of the primary dispersion at 10 Hz is recognized as T_g
[b] k_D = Henry's law solubility coefficient
[c] C'_H = Langmuir sorption capacity or hole saturation constant
[d] b = affinity constant of Langmuir site

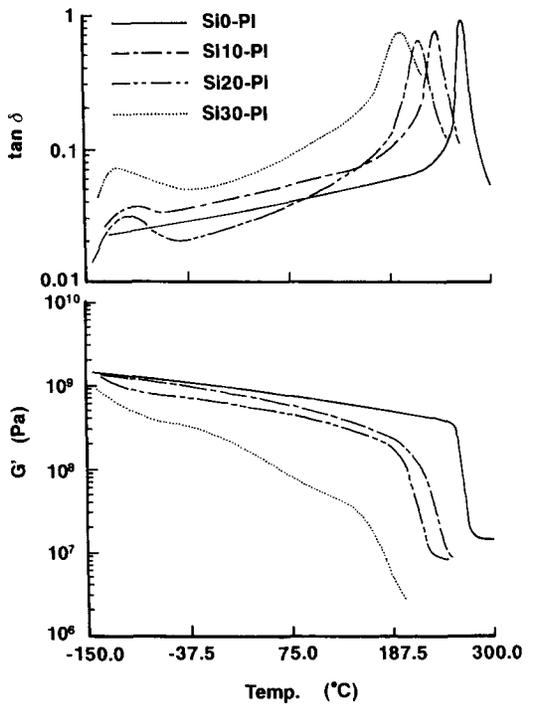

Figure 1 Temperature dispersion of shear modulus (G') and loss tangent (tan δ) at a frequency of 10 Hz for Si0–PI, Si10–PI, Si20–PI and Si30–PI membranes

dispersion of the PAA phase (see *Table 1*), is not observed in each tan δ curve, indicating that imidization was complete under the experimental conditions in this study. The primary dispersion temperature of the PI-rich phase is decreased and the width of the peak is broadened with increasing PDMS content. In contrast, the tan δ peaks observed at about −110°C, which correspond to primary dispersion of the PDMS phase, are almost independent of the PDMS content. These findings show that PDMS dissolves in the PI phase to some extent with increasing PDMS content. However, we emphasize the fact that two tan δ peaks were observed for Sixx–PI membranes. This fact is obvious proof that Sixx–PI membranes consist mainly of a microphase separated structure of PI-rich and PDMS phases.

The values of G' below the primary dispersion of Sixx–PI membranes are gradually decreased with the PDMS content. It can be said that the introduction of PDMS into PI slightly influences the modulus of the block copolymers.

The data of Si0–PAA and Si20–PAA membranes whose T_g differ greatly from those of Si0–PI and Si20–PI membranes are also shown in *Table 1*. The effect of PDMS on the T_g of the PI-rich phase is larger than on that of the PAA phase, reflecting the difference between miscibilities for PDMS of PI and PAA phases.

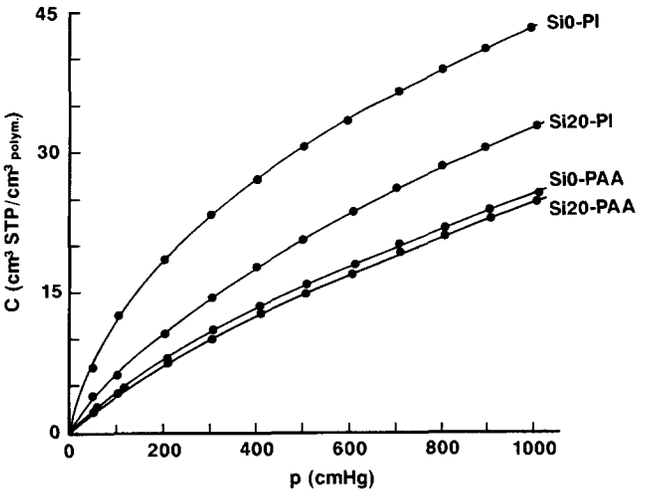

Figure 2 CO_2 sorption isotherms of Si0–PAA, Si0–PI, Si20–PAA and Si20–PI membranes at 25°C. The circles are experimental data and the full curves correspond to the calculated curves based on the dual-mode sorption model (equation (1))

Sorption properties

Figure 2 shows the CO_2 sorption isotherms of Si0–PAA, Si0–PI, Si20–PAA and Si20–PI membranes at 25°C, where C is the total CO_2 concentration and p is the pressure of CO_2. The amount of CO_2 sorption increases with imidization, and decreases with the introduction of PDMS, reflecting the T_g and the less-sorptive capability of the siloxane group. Each isotherm shown in *Figure 2* can be described fairly well by the dual-mode sorption model, which is represented by the following equation[16,17]:

$$C = C_D + C_H = k_D p + (C'_H b p)/(1 + bp) \quad (1)$$

Here C_D is the concentration due to Henry's law contribution, C_H is the concentration due to Langmuir-mode contribution, k_D is the Henry's law solubility coefficient, b is the affinity constant of penetrant to the Langmuir site, and C'_H is the hole saturation constant in the Langmuir sorption mode. The dual-mode sorption parameters were evaluated using the non-linear least-squares method, and the parameters obtained are listed in *Table 1*. The values of C'_H are changed greatly compared with the changes in the values of k_D. The changes in the amount of CO_2 sorption, therefore, can be mainly represented in terms of the changes in C'_H.

In general, Langmuir-mode sorption is interpreted by the sorption of CO_2 gas with a liquid-like volume into an unrelaxed volume and/or a microvoid of glassy polymers. Namely, C'_H is represented using the unrelaxed volume by the following equation[18–20]:

$$C'_H = 22\,400[(V_g - V_l)/V_g]/V_{CO_2} \quad (2)$$

where $(V_g - V_l)/V_g$ is the unrelaxed volume fraction, the ratio of the difference between the observed specific volume in the glassy state (V_g) and the volume in the supercooled equilibrium liquid state (V_l) to V_g, and V_{CO_2} is the molar volume of liquid-like CO_2 in the Langmuir sorption site. The unrelaxed volume fraction can also be related to T_g by the following expression:

$$(V_g - V_l)/V_g = (\alpha_l - \alpha_g)(T_g - T)/[1 - \alpha_g(T_g - T)]$$
$$\simeq (\alpha_l - \alpha_g)(T_g - T) \quad (3)$$

where α_l and α_g are the thermal expansion coefficients for liquid and glassy states, respectively. Now, the equation of C'_H, equation (2), is rewritten with equation (3) as follows:

$$C'_H = 22\,400(\alpha_l - \alpha_g)(T_g - T)/V_{CO_2} \quad (4)$$

where T is the temperature of the sorption experiment. It has been reported[18–21] that C'_H of common glassy polymers is approximately proportional to $(T_g - T)$. *Figure 3* shows the plot of C'_H at 25°C *versus* T_g for Si0–PAA, Si0–PI, Si20–PAA and Si20–PI membranes. For Si0–PAA and Si0–PI membranes, it can be seen that the relationship between C'_H and T_g satisfies equation (4), and a reasonable straight line is obtained that intercepts the abscissa, i.e. $C'_H = 0$. The observed values of Si20–PAA and Si20–PI membranes deviate from the line. Since the Langmuir site does not exist in rubbery polymers, the values of C'_H for Si20–PAA and Si20–PI membranes determined from the sorption isotherms should be corrected by considering only the volume of the glassy phase. Assuming that the glassy phase is simply composed of PAA or PI component, the volume fractions of glassy phase for Si20–PAA and Si20–PI membranes were determined using the densities of Si0–PAA, Si0–PI and PDMS membranes, and then the correction of the observed C'_H was carried out. The corrected C'_H for Si20–PAA and Si20–PI membranes are plotted in *Figure 3* as triangles. These corrected values do fit the line, although the volume fraction of glassy phase was estimated roughly. This finding indicates that

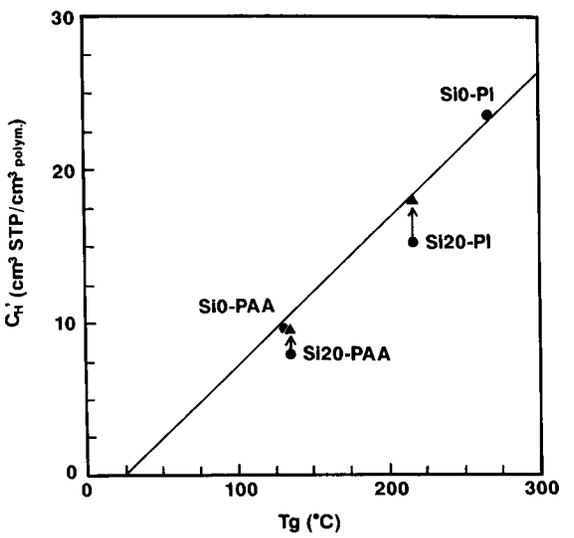

Figure 3 Langmuir sorption capacity terms (C'_H) for CO_2 in Si0–PAA, Si0–PI, Si20–PAA and Si20–PI membranes at 25°C as a function of the glass transition temperature T_g (primary dispersion temperature). The circles are the data of *Table 1*, and the triangles are the corrected data by considering the volume fraction of PI phase in the membrane. Details are described in the text

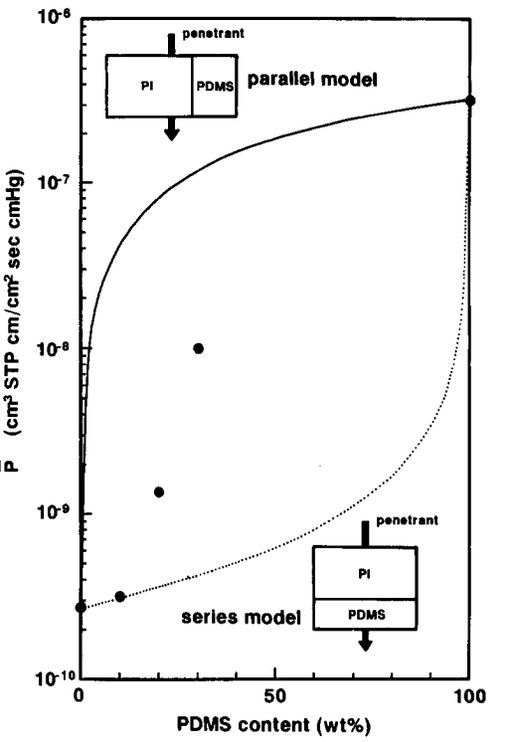

Figure 4 Permeability coefficient of CO_2 for Si0–PI, Si10–PI, Si20–PI and Si30–PI membranes at 25°C as a function of PDMS content. The upstream pressure is about 200 cmHg. The value for a PDMS membrane[22] is also shown in this plot. The full and dotted curves are the calculated curves based on the parallel (equation (5)) and series (equation (6)) models, respectively

the glassy and rubbery phases in these membranes can be clearly distinguished from each other.

Permeation properties

The permeability coefficient of CO_2 ($\bar{P}_{CO_2}$) at 25°C was measured. *Figure 4* shows $\bar{P}_{CO_2}$ for Si0–PI, Si10–PI, Si20–PI and Si30–PI membranes at an upstream pressure of about 200 cmHg together with that for PDMS membrane[22]. A slight effect of the PDMS content on permeability is observed for Si10–PI membrane, and $\bar{P}_{CO_2}$ for Si20–PI and Si30–PI membranes is increased remarkably with PDMS content. In the discussion of sorption behaviour mentioned above, one does not need to consider the arrangement of glassy and rubbery phases. However, permeation behaviour depends strongly on the arrangement of glassy and rubbery phases. The following simple structural model is, therefore, proposed to understand qualitatively the permeation behaviour of the block copolymer, although one has to discuss the relationship between detailed structural model and permeation behaviour. Since Six*x*–PI membranes mainly consisted of PI and PDMS phases, the relationship between $\bar{P}_{CO_2}$ and PDMS content based on two types of two-phase model is considered. One is the parallel model, in which PI and PDMS phases are arranged parallel to the direction of permeation of the penetrant, and the other is the series model, in which the two phases are arranged perpendicular to it (see *Figure 4*). In the parallel model, the total permeability coefficient $\bar{P}$ is represented by:

$$\bar{P} = \phi_{PI}\bar{P}_{PI} + \phi_{PDMS}\bar{P}_{PDMS} \quad (5)$$

where ϕ_{PI} and ϕ_{PDMS} are the volume fractions of PI and PDMS phases, respectively, and $\bar{P}_{PI}$ and $\bar{P}_{PDMS}$ are the

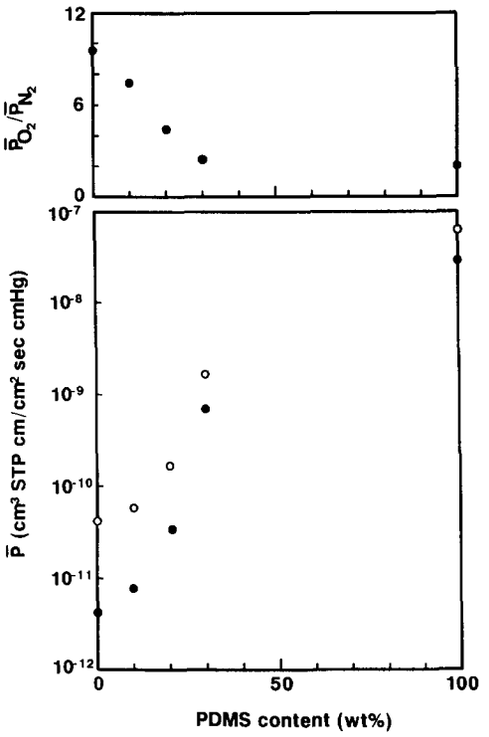

Figure 5 Permeability coefficients of O_2 (○) and N_2 (●) and its selectivity $\bar{P}_{O_2}/\bar{P}_{N_2}$ for Si0–PI, Si10–PI, Si20–PI and Si30–PI membranes at 25°C as a function of PDMS content. The upstream pressure is about 200 cmHg. The data for a PDMS membrane[22] are also shown in these plots

permeability coefficients for PI and PDMS phases, respectively. In the case of the series model, $\bar{P}$ is given by:

$$1/\bar{P} = \phi_{PI}/\bar{P}_{PI} + \phi_{PDMS}/\bar{P}_{PDMS} \quad (6)$$

Figure 4 shows the curves calculated based on the parallel and series models using the values of $\bar{P}_{CO_2}$ and the densities of Si0–PI and PDMS membranes. It can be seen that the Si10–PI membrane takes the structure corresponding to the series model. However, the values of $\bar{P}_{CO_2}$ for Si20–PI and Si30–PI membranes deviate from the series model curve towards the parallel one. This finding shows that the region of the structure that should be interpreted by the parallel model increases with the PDMS content.

Next, the permselectivity of O_2 to N_2 is discussed. The permeability coefficients of O_2 ($\bar{P}_{O_2}$) and N_2 ($\bar{P}_{N_2}$) and the ratio of $\bar{P}_{O_2}$ to $\bar{P}_{N_2}$ ($\bar{P}_{O_2}/\bar{P}_{N_2}$) at 25°C for Si0–PI and Si*xx*–PI membranes as a function of the PDMS content are shown in *Figure 5*, together with the data of PDMS[22]. The values of both $\bar{P}_{O_2}$ and $\bar{P}_{N_2}$ increase with the PDMS content as well as the case of $\bar{P}_{CO_2}$. Especially, these values increase remarkably when the PDMS content is more than 10 wt%. On the other hand, $\bar{P}_{O_2}/\bar{P}_{N_2}$ decreases with increasing PDMS content, and the value for Si30–PI membrane becomes almost equal to that of PDMS. We calculated $\bar{P}_{O_2}$ and $\bar{P}_{N_2}$ by using the parallel and series models, and then the values of $\bar{P}_{O_2}/\bar{P}_{N_2}$ based on these models were determined as functions of the PDMS content. The results of the calculations show that the permselectivity of O_2 to N_2 is strongly dependent on the arrangement of the two phases. That is, $\bar{P}_{O_2}/\bar{P}_{N_2}$ based on the parallel model is suddenly decreased with a slight amount of PDMS, but that based on the series model is scarcely decreased up to considerably higher content of PDMS. For example, when the PDMS content is 2.5 wt%, $\bar{P}_{O_2}/\bar{P}_{N_2}$ based on the parallel model already becomes 2.1, which is almost the same as that of the PDMS membrane. In the series model, the calculated $\bar{P}_{O_2}/\bar{P}_{N_2}$ are more than 9.2 even if the PDMS content was 97.5 wt%. This value (9.2) is very close to that of Si0–PI membrane (9.5). Therefore, the fact that $\bar{P}_{O_2}/\bar{P}_{N_2}$ decreases with increasing PDMS content should also be interpreted by considering the arrangement of the two phases in Si*xx*–PI membranes as well as the case of the permeation coefficients.

CONCLUSION

Si*xx*–PI membranes consist of a microphase separated structure, and have both the mechanical properties of PI and the high gas permeability of PDMS. The mechanical properties of Si*xx*–PI membranes are well retained up to a PDMS content of about 20 wt%. The sorption behaviour of Si*xx*–PI membranes is interpreted in terms of the dual-mode sorption theory, which is applied to the glassy phase. In order to understand the permeation and permselectivity behaviour of Si*xx*–PI membranes, not only the compositions of the glassy and rubbery phases but also their arrangement must be considered. It is concluded that the permeability and permselectivity of Si*xx*–PI membranes are found to be controlled by the PDMS content.

REFERENCES

1 Allen, S. M., Fujii, M., Stannett, V., Hopfenberg, H. B. and Williams, J. L. *J. Membr. Sci.* 1977, **2**, 153
2 Minoura, N., Tani, S. and Nakagawa, T. *J. Appl. Polym. Sci.* 1978, **22**, 883
3 Ward, III, W. J., Browall, W. R. and Sallemme, R. M. *J. Membr. Sci.* 1976, **1**, 99
4 Asakawa, S., Saito, Y., Kawahito, M., Itoh, Y., Tsuchiya, S. and Sugata, K. *Natl. Tech. Rep.* 1983, **29**, 93
5 Stern, S. A., Shah, V. M. and Hardy, B. J. *J. Polym. Sci., Polym. Phys. Edn.* 1987, **25**, 1263
6 Hachisuka, H., Goto, S., Tsujita, Y., Takizawa, A., Kinoshita, T. and Miyamoto, M. *Polymer* 1990, **30**, 276
7 McCandless, F. P. *Ind. Eng. Chem., Process. Des. Dev.* 1972, **11**, 470
8 Haraya, K., Obata, K., Hakura, T. and Yoshitome, H. *Membrane* 1986, **11**, 48
9 Koros, W. J., Patton, C. J., Felder, R. M. and Finder, S. J. *J. Polym. Sci., Polym. Phys. Edn.* 1980, **18**, 1485
10 Felder, R. M., Patton, C. J. and Koros, W. J. *J. Polym. Sci., Polym. Phys. Edn.* 1981, **19**, 1895
11 Chern, R. T., Koros, W. J., Yui, B., Hopfenberg, H. B. and Stannet, V. T. *J. Polym. Sci., Polym. Phys. Edn* 1984, **22**, 1061
12 Uragami, T., Hopfenberg, H. B., Koros, W. J., Yang, D. K., Stannet, V. T. and Chern, R. T. *J. Polym. Sci., Polym. Phys. Edn.* 1986, **24**, 779
13 Hachisuka, H., Tsujita, Y., Takizawa, A. and Kinoshita, T. *Polym. J.* 1989, **21**, 681
14 Hachisuka, H., Tsujita, Y., Takizawa, A. and Kinoshita, T. *Polym. J.* 1989, **21**, 1019
15 Hachisuka, H., Tsujita, Y., Takizawa, A. and Kinoshita, T. *J. Polym. Sci., Polym. Phys. Edn.* 1991, **29**, 11
16 Michaels, A. S., Vieth, W. R. and Barrie, J. A. *J. Appl. Phys.* 1963, **34**, 1
17 Michaels, A. S., Vieth, W. R. and Barrie, J. A. *J. Appl. Phys.* 1963, **34**, 13
18 Wonders, A. G. and Paul, D. R. *J. Membr. Sci.* 1979, **5**, 63
19 Koros, W. J. and Paul, D. R. *Polym. Eng. Sci.* 1980, **20**, 14
20 Masi, P., Paul, D. R. and Barlow, J. W. *J. Polym. Sci., Polym. Phys. Edn.* 1982, **20**, 15
21 Hachisuka, H., Sato, T., Tsujita, Y., Takizawa, A. and Kinoshita, T. *Polym. J.* 1989, **21**, 417
22 Yasuda, H. and Resoengren, K. J. *J. Appl. Polym. Sci.* 1970, **14**, 2839